A New Soft-Switched DC-DC Converter

Majid Pakdel, Rogayeh Purabbasali and Samira Fareghi
Islamic Azad University, Miyaneh Branch
majidpakdel@yahoo.com, luka_elen@yahoo.com, fareghi_s@yahoo.com

Abstract- **In a two-quadrant soft-switching (TQSS) converter, there are no switches available for current boosting because it uses diodes in the current return path. Therefore, a new control-timing scheme is proposed in this TQSS converter with only one auxiliary branch to achieve near zero-voltage switching under all load-conditions. In order to validate the proposed converter, computer simulations and experimental results were conducted. With the merits of simplicity and flexibility, the proposed TQSS converter shows excellent performance and potential for various industry applications including switched reluctance motor (SRM) drives, high-frequency-high-voltage choppers, magnet drivers, and magnetic resonance imaging (MRI) system applications.**

Fig. 1. Proposed two-quadrant soft-switching converter.

I. INTRODUCTION

There has been an increasing interest in the soft-switching power conversion technologies in order to overcome the limitations of the hard-switching technologies [1]-[7]. Soft-switching (SS) converters had many advantages over hard-switching (HS) converters. For example, SS converters lower switching losses, reduce voltage/current stress, reduce EMI, and allow a greater high switching frequency in high power applications [1]. Despite the advantages of SS converters, its applications have been so far limited due to complexity in the design of SS circuits, and difficult in control realization. There has been a growing demand for a simple design that provides reliable control in a wide-range of operational condition. Several SS techniques have been developed such as the auxiliary resonant snubber inverter (RSI) [1], the auxiliary resonant commutated pole inverter (ARCP) [3], [6], the inductor coupled zero-voltage transition inverter (ZVT) [4]-[5], and the resonant dc link inverter (RDCL) [2], [7], [8]. The RSI is suitable for single or three-phase inverters with multiple branches of auxiliary circuits but needs modification of space vector modulation to ensure zero voltage switching. The ARCP requires large split capacitors to achieve a zero-voltage switching. The ZVT requires bulky coupled inductors to reset the resonant current. The RDCL needs a device voltage rating higher than that which has been used in other converters. This study found that the RSI can easily be extended to two-quadrant chopper applications, but it must use a variable boost current to meet different load current conditions. In a two-quadrant soft-switching (TQSS) converter, there are no switches available for current boosting because it uses diodes in the current return path. Therefore, a new control-timing scheme is proposed in this TQSS converter with only one auxiliary branch to achieve near zero-voltage switching under all load-conditions. In order to validate the proposed converter,
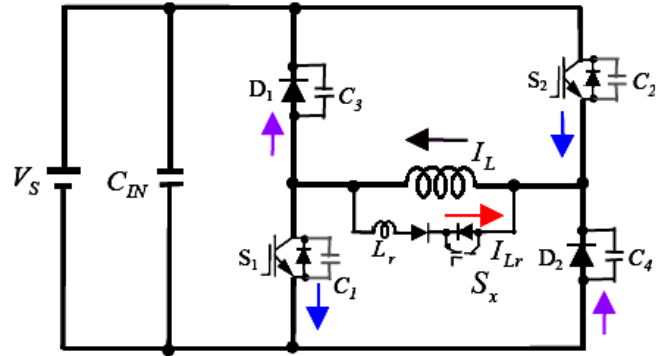
computer simulations and experimental results were conducted. The proposed converter has better operation with respect to the converters described in [9-17]. In the simulation and experimental results, the purpose of the comparison between soft-switching and hard-switching was to investigate the following characteristics: the voltage spike, EMI noise, turn-off dv/dt, heat sink temperature, power loss and control flexibility. With the merits of simplicity and flexibility, the proposed TQSS converter shows excellent performance and potential for various industry applications including switched reluctance motor (SRM) drives, high-frequency-high-voltage choppers, magnet drivers, and magnetic resonance imaging (MRI) system applications.

II. PROPOSED CONVERTER TOPOLOGY AND ITS OPERATIONS

A. Operation Principles

Fig. 1 shows the proposed two-quadrant soft-switching converter consisting of a pair of switches (S1 and S2), a pair of diodes (D1 and D2), and one auxiliary switch. The two switches are synchronously conducting or blocking depending on the desired switching duties. Two diodes provide a freewheeling current path and a reverse voltage across the load to form a two-quadrant operation. Notice that the load current is unidirectional. When the load current is flowing in diodes D1 and D2, turning on S1 and S2 would shut off the diode current, but on the other hand, produce a large diode reverse recovery current and turn-on loss. Snubber capacitors are added across the main devices to reduce turn off losses. The auxiliary branch is connected between the two phase-legs or across the load. This branch consists of one auxiliary switch, one fast recovery diode, and one resonant inductor. Fig. 2 shows the key operating waveforms of the proposed converter circuit.
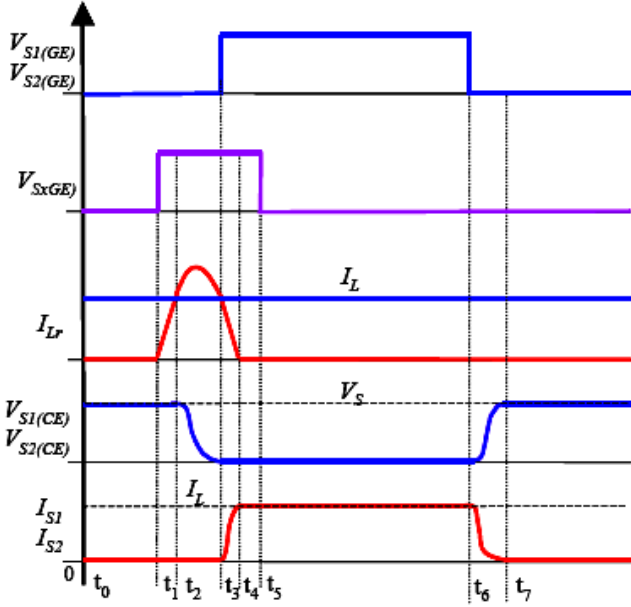
Fig. 2. Operational waveforms of the proposed converter.

B. Circuit Analysis

For a simple circuit analysis, it is assumed that the load current remains constant during the one-cycle operation as shown in Fig. 2. Under this assumption, analysis is performed on the circuit for seven distinct operating modes in the period [t0 - t7]. Initially at time t0, all the switches are off, and load current flows through D1 and D2.

Mode M0 (t0 – t1): Assuming that the load current is positive, the free-wheeling diodes D1 and D2 conduct the load current, and the main devices are off.

Mode M1 (t1 – t2): After the auxiliary switch, Sx, turns on, the inductor current, I_{Lr}, increases linearly until it equals the load current I_L. At this time, the current through D1 and D2 starts to decrease slowly to zero. The slope can be determined as a function of the resonant inductor and dc source as shown below.

$$\frac{di_{Lr}}{dt} = \frac{V_S - V_D}{L_r} \qquad (1)$$

where V_D is the total conducting voltage across the switching devices. At time t2, the resonant inductor current I_{Lr} equals the load current I_L and the diode currents reach zero. The charging time is calculated using:

$$t_2 - t_1 = \frac{L_r \cdot I_L}{V_S} \qquad (2)$$

In order to meet the energy balance requirement for the resonant components, the aforementioned energy requirement can be represented in (3):

$$\frac{1}{2} L_r (I_{Lr} - I_L)^2 \geq C_r (V_S - V_D)^2 \qquad (3)$$

where Cr is the equivalent resonant capacitance of the snubber capacitors, when C1=C2=C3=C4=Cr. This relationship

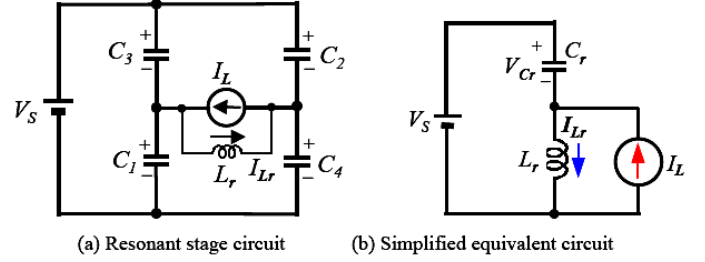(a) Resonant stage circuit   (b) Simplified equivalent circuit
Fig. 3. Equivalent circuit during resonant mode.

indicates that the resonant capacitors, which are across the main devices, are either fully charged or discharged during resonance.

Mode M2 (t2 – t3): The diodes, D1 and D2, are turned off naturally, when the resonant current is larger than the load current. The resonant capacitor and inductor resonate to discharge the capacitor voltage across the main switches. At time t2, the initial device voltages, V_{S1} and V_{S2}, are equal to V_S. Fig. 3 shows the equivalent circuit during **M2** mode, where the inductor is replaced by a current source, I_L. The initial value for the inductor current, I_{Lr}, is I_L, and for the resonant capacitor voltage, V_{Cr}, is V_S. Under these conditions, the resonant capacitor voltage and inductor current can be expressed as:

$$\begin{cases} V_{Cr}(t) = V_S \cdot (1 - \cos(wt)) \\ I_{Lr}(t) = I_L + \frac{V_S}{Z_r} \sin(wt) \end{cases} \qquad (4)$$

where:

$$w_r = \frac{1}{\sqrt{L_r \cdot C_r}}, \ Z_r = \sqrt{\frac{L_r}{C_r}} \qquad (5)$$

At time t3, when the resonating cycle begins, V_{Cr} reaches zero and the parallel diodes of S1 and S2 provide a path for the resonant-current to control. The capacitor across the switch discharges at a finite rate allowing the switch voltage to drop to zero.

Mode M3 (t3 – t4): By the end of the resonant period, t3, the snubber capacitors are discharged to zero voltage. At this moment, the main switch can be turned on easily under zero-voltage condition. Without extravagant sensing, it is difficult to turn on the main switch at the exact moment the capacitor voltage drops to zero. Therefore, the main switch can only be turned on under a near-zero-voltage condition. When the main switches turn on, the inductor current decreases linearly due to reverse voltage polarity of the opposite diode.

Mode M4 (t4 – t5): The resonant current decreases until it hits zero at t4. The auxiliary switch and diode are then turned off under zero-current condition at t5. The main switches now conduct the load current. The auxiliary switch and diode are both turned off after time t4.

Mode M5 (t6 - t7): After the steady-state, (t5-t6), the main switches turn off without loss using snubber capacitors, which
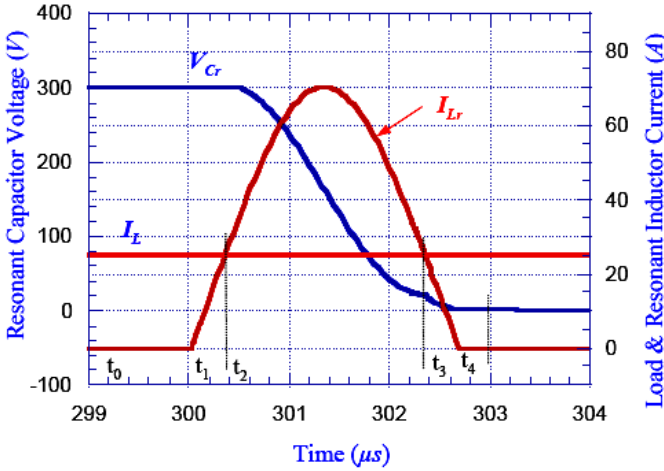
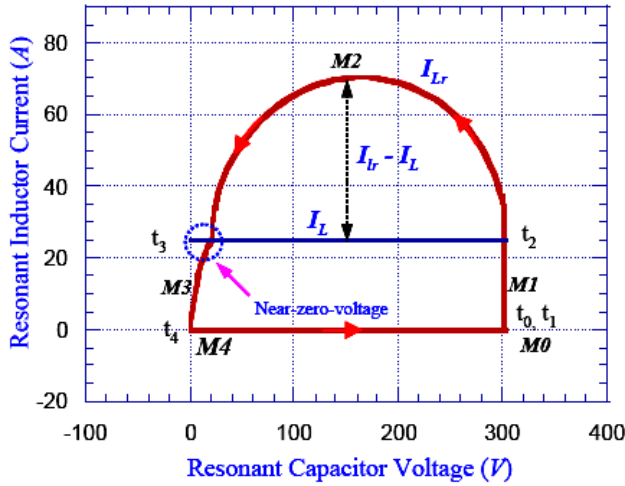Fig. 4. Simulated current and voltage waveforms of the converter under soft-switching.

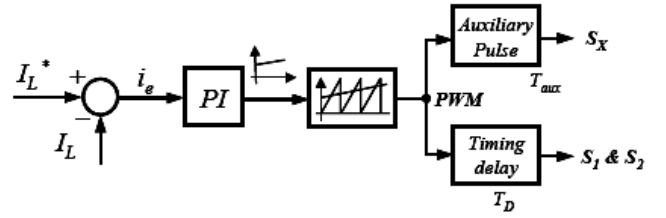Fig. 5. Soft-switching state-plane trajectory diagram.

(a) Soft-switching control scheme

(b) Gate signals

Fig. 6. Control block diagram under soft-switching.

M1 and discharging modes M3 increase. The selection of the resonant capacitor is very crucial for proper operation of the circuit, because the resonant capacitor reduces the turn-off loss and turn-off dv/dt of the device. A larger size capacitor can reduce the turn-off loss and dv/dt. However, the extra energy stored in the resonant capacitor needs to be discharged during turn on. So, the capacitor size should be optimized so that both turn-on and turn-off losses are reduced. The rate of change of voltage across the resonant capacitor can be expressed as:

$$\frac{dV_{CE}}{dt} = \frac{I_{SW}}{C_r} \qquad (6)$$

where, V_{CE} is the collect-emitter voltage, and I_{SW} is the device current, which equals to the load current, I_L, during switching. After selecting the resonant capacitor, the resonant inductor should be designed based on peak resonant current and the time to reach peak resonant current. These two factors can also be translated into the resonant tank impedance Zr $(= \sqrt{L_r/C_r})$ and its resonant frequency fr $(= 1/2\pi\sqrt{L_rC_r})$. Using the values selected for the resonant capacitor and inductor, the auxiliary switch conduction time T_{aux} is as follows:

$$T_{aux} = 2((L_r.I_L)/V_S + \pi\sqrt{L_r.C_r}) \qquad (7)$$

B. Control Flexibility

The proposed converter has a very flexible control scheme for wide variation in load current. This is because the resonant current follows the load current. Fig. 6 shows the control block diagram of the converter and its gate signals for soft-switching operations. The gate signals for the S1 and S2 have a time
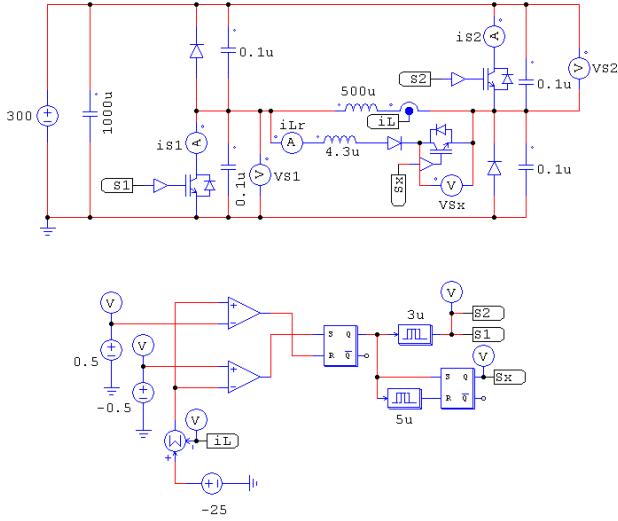
carry the load current until diodes D1 and D2 turn on and the operation returns to **M0**.

III. CONVERTER CHARACTERISTICS

In This study, the proposed TQSS converter is characterized and modeled the converter's control flexibility by using PSIM circuit simulator.

A. Soft-Switching State-Plane Trajectory

In order to design the soft-switching circuit, the state plane trajectory diagram can be used widely. Fig. 4 shows the key waveforms of the proposed converter when the dc bus voltage is 300-V and the load current is 25-A. It can be seen that the main switches operate well under near zero-voltage condition. Fig. 5 shows the state-plane trajectory for the same operating conditions. This diagram explains operational modes of the proposed converter. It is clear that the resonant tank impedance is independent of the load current condition as shown in (Fig. 4). The peak value of the resonant current is ($I_{Lr} - I_L$). As the load current increases the duration of the pre-charging modes

Fig. 7. Proposed two quadrant soft switched converter in PSIM software.

Vo = 2V, load current of 0.4A and a switching frequency of 50 kHz. The clock signal in a time period of one switching cycle is shown in Fig. 11. The V_{DS} waveforms of switches S_1, S_2 and S_X in a time period of one switching cycle are shown in Fig. 12, Fig. 13, and Fig. 14 respectively. The output DC current is shown in Fig. 15.
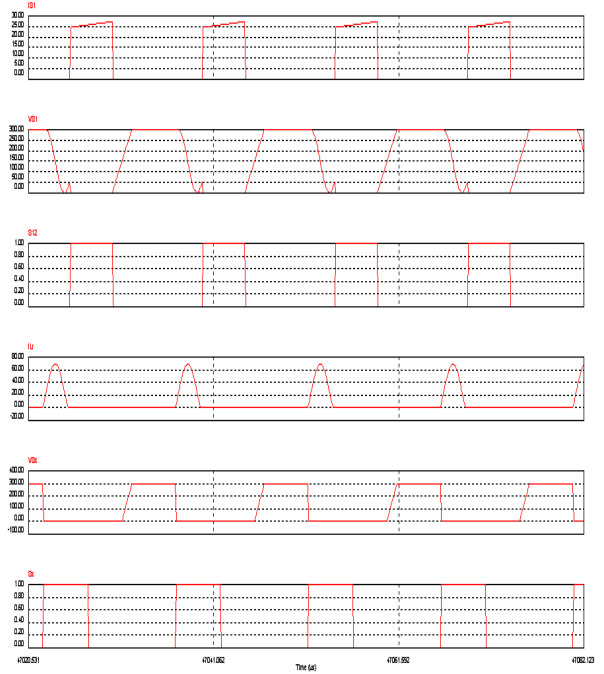

Fig. 8. Waveforms of i_{S1}, v_{S1}, S_1, i_{Lr}, v_{Sx}, S_x.

delay of T_D, and the S_X signal has a fixed short pulse of T_{aux} generated by the PWM signal, whenever the rising edge on the PWM signals through the proportional-integrated (PI) current controller occurs. The parameters used in the experiment are explained as the following section.

IV. SIMULATION RESULTS

The proposed two quadrant soft switched converter in the PSIM software environment is shown in Fig. 7. The following circuit parameters have been used in simulations:

1) A dual IGBT module at 600V - 200A was used;
2) The resonant capacitors used were $0.1\mu F$ - 600V Polypropylene capacitors;
3) The resonant inductor used was $4.3\mu H$;
4) The auxiliary switch chosen was a 50A - 600V IGBT;
5) The blocking auxiliary diode was chosen as an HFA50PA60C rated at 50A - 600V; and
6) The auxiliary conducting time used was $5\mu S$.

The waveforms of i_{S1}, v_{S1}, S_1, i_{Lr}, v_{Sx}, S_x are shown in Fig. 8 also the wave form of i_L is shown in Fig. 9. The simulation results show that the proposed two quadrant soft switched converter has the proper response and the current i_L is very easily controlled using hysteresis control method.

V. EXPERIMENTAL RESULTS

A Prototype of the proposed converter, as shown in Fig. 10 has been built in the laboratory. The newly proposed converter operates with an input voltage Vs = 6V, output voltage
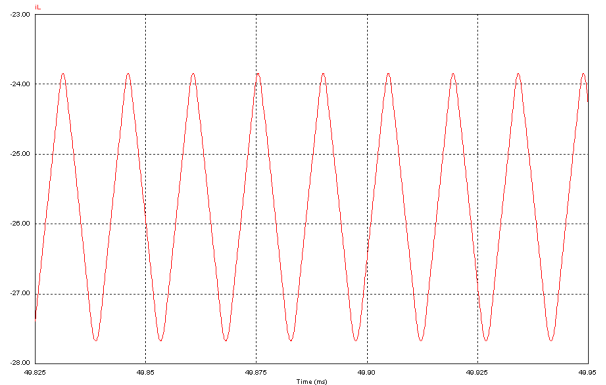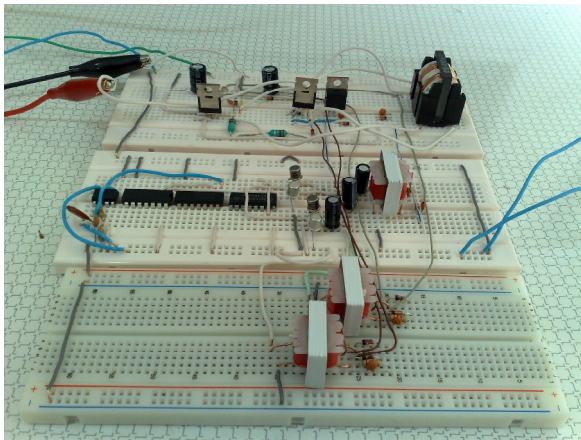

Fig. 9. Waveform of i_L.
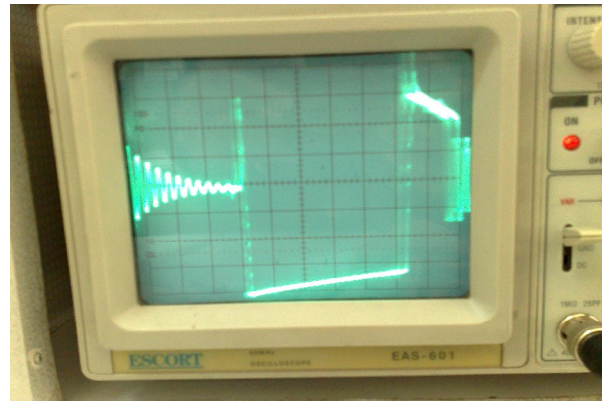
Fig. 10. Prototype of the proposed converter.

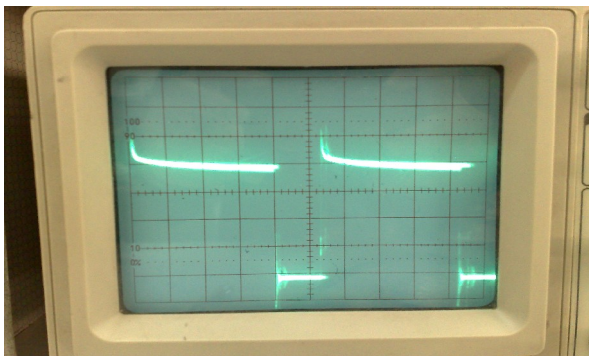Fig.13 . The V_{DS} waveforms of switch S_2 Volt/Div 1v, Time/Div 5us.

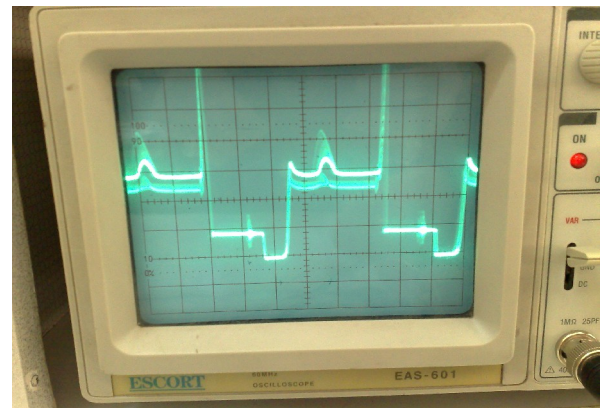Fig.11 . The clock signal, Volt/Div 2v, Time/Div 5us.

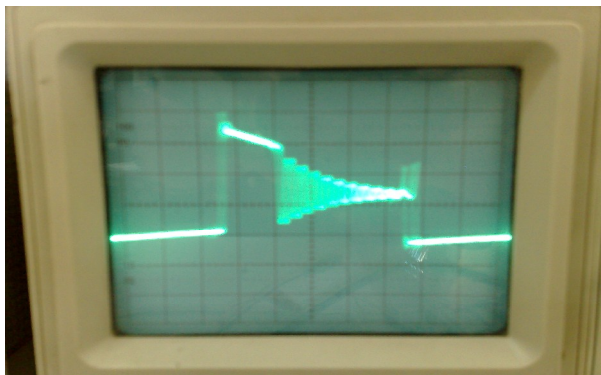Fig.14 . The V_{DS} waveforms of switch S_X Volt/Div 2v, Time/Div 5us.

Fig.12 . The V_{DS} waveforms of switch S_1, Volt/Div 2v , Time/Div 5us.
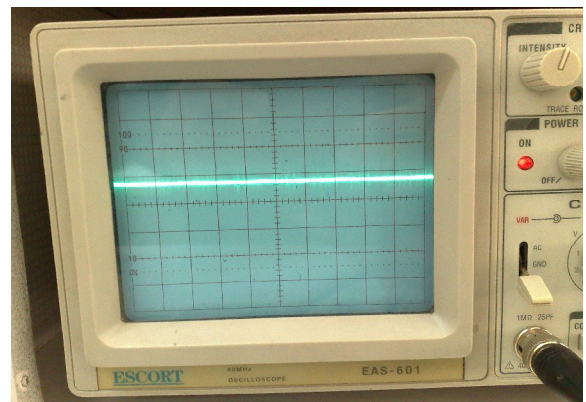

Fig.15 . The output DC current Volt/Div 2v, Time/Div 20us.

VI. Conclusion

In this section, a new soft-switching converter topology with a simple resonant snubber circuit was proposed and was verified fully for working conditions with an inductive load. In order to verify performance of the proposed converter, circuit simulations using PSIM software and experimental results were given. With the merits of simplicity and flexibility, the proposed TQSS converter shows excellent performance and potential for various industry applications including switched reluctance motor (SRM) drives, high-frequency-high-voltage choppers, magnet drivers, and magnetic resonance imaging (MRI) system applications.

REFERENCES

[1] J. S. Lai, R. W. Young, G. W. Ott, J. W. McKeever, and F. Z. Peng, "A Delta Configured Auxiliary Resonant Snubber Inverter," *IEEE Trans. on Ind. Appl.*, Vol. 32, No. 3, May/Jun. 1996, pp. 518–525.

[2] D. M. Divan, "The Resonant DC Link Converter -- A New Concept in Static Power Conversion," in *Conf. Rec. of IEEE-IAS*, Oct. 1986, pp. 648-656.

[3] W. McMurray, "Resonant Snubbers with Auxiliary Switches," *IEEE Trans. on Ind. Appl.*, Vol. 29, No. 2, Mar./Apr. 1993, pp. 355–362.2.

[4] H. Mao and F. C. Lee, "Improvement on Zero-Voltage Transition Three-Phase Rectifier/Inverter," in *Proc. of VPEC'95 Seminar*, Vol. 13, 1995, pp. 19-27.

[5] J. P. Gegner and C. Q. Lee, "Zero-Voltage Transition Converters using Inductor Feedback Technique," in *Conf. Rec. of IEEE-APEC*, Orlando, FL, Mar. 1994, pp. 862-868.

[6] R. W. De Doncker and J. P. Lyons, "The Auxiliary Resonant Commutated Pole Converters*," in *Conf. Rec. of IEEE-IAS,* 1990, pp. 1228-1235.

[7] J. He and N. Mohan, " Parallel Resonant DC Link Circuit – A Novel Zero Switching Losses Topology with Minimum Voltage Stresses," in *Conf. Rec. of IEEE-PESC*, 1989, pp. 1006- 1012.

[8] R. Redl, N. O. Sokal, and L. Balogh, "A novel soft-switching full-bridge dc/dc converter: Analysis, design considerations, and experimental results at 1.5 kW, 100 kHz," *IEEE Trans. Power Electron.*, vol. 6, no. 3, pp. 408− 418, Jul. 1991.

[9] B. Choi,W. Lim, S. Bang, and S. Choi, "Small-signal analysis and control design of asymmetrical half-bridge DC-DC converters," *IEEE Trans. Ind. Electron.*, vol. 53, no. 2, pp. 511–520, Apr. 2006.

[10] J.-J. Lee and B.-H. Kwon, "DC-DC converter using a multiple-coupled inductor for low output voltages," *IEEE Trans. Ind. Electron.*, vol. 54, no. 1, pp. 467–478, Feb. 2007.

[11] S.-S. Lee, S.-K. Han, and G.-W. Moon, "Analysis and design of asymmetrical ZVS PWM half bridge forward converter with flyback type transformer," in *Proc. IEEE Power Electron. Spec. Conf.*, 2004, vol. 2, pp. 1525–1530.

[12] L. H. Dixon, "Magnetics design for switching power supplies," *Unitrode Seminar*, 2001.

[13] Kh. Rahimi kh., M. Pakdel, "A New ZVZCS Isolated DC-DC Converter," in Proc. IEEE ICIT2009. Conf., Australia, Feb. 2009.

[14] Y.Chul Ryu; Y.Woong Hwang, "A new soft-start method with abnormal over current protection function for switching power supplies ," IEMDC.2005.195757, 2005, pp. 421-425.

[15] Konishi, Y., Huang, Y.F., "Soft-switching buck boost converter using pulse current regenerative resonant snubber," IET, 2007, pp. 127-128.

[16] Barreto, L.H.S.C., Sebastiao, M.G., de Freitas, L.C., Coelho, E.A.A., Farias, V.J., Vieira, J.B., Jr., "Analysis of a soft-switched PFC boost converter using analog and digital control circuits," IEEE Trans. Ind. Elect., 2005, pp. 221-227.

[17] Dong Cao; Fang Zheng Peng, "A family of zero current switching switched-capacitor dc-dc converters," APEC.2010.5433407, 2010, pp. 1365-1372.